Journal of Thermal Science Vol.19, No.3 (2010) 245−252

DOI: 10.1007/s11630-010-0245-8 **Article ID: 1003-2169(2010)03-0245-08**

Development and Testing of Aluminum Micro Channel Heat Sink

G.Kumaraguruparan and T.Sornakumar

Department of Mechanical Engineering, Thiagarajar College of Engineering, Madurai-625015, India

Microchannel heat sinks constitute an innovative cooling technology for the removal of a large amount of heat from a small area and are suitable for electronics cooling. In the present work, Tool Steel D2 grade milling slitting saw type plain milling cutter is fabricated The microchannels are machined in aluminum work pieces to form the microchannel heat sink using the fabricated milling cutter in an horizontal milling machine. A new experimental set-up is fabricated to conduct the tests on the microchannel heat sink. The heat carried by the water increases with mass flow rate and heat input. The heat transfer coefficient and Nusselt number increases with mass flow rate and increased heat input. The pressure drop increases with Reynolds number and decreases with input heat. The friction factor decreases with Reynolds number and decreases with input heat. The thermal resistance decreases with pumping power and decreases with input heat.

Keywords: Microchannel, heat transfer, pressure drop, friction factor, heat transfer coefficient.

Introduction

Microchannel heat sinks constitute an innovative cooling technology for the removal of a large amount of heat from a small area. The heat sink is usually made from a high thermal conductivity solid such as silicon or copper with the microchannels fabricated into its surface by either precision machining or microfabrication technology. These microchannels have characteristic dimensions ranging from 10 to 1000 μm, and serve as flow passages for the cooling liquid. Microchannel heat sinks combine the attributes of very high surface area to volume ratio, large convective heat transfer coefficient, small mass and volume, and small coolant inventory. These attributes render these heat sinks very suitable for cooling such devices as high-performance microprocessors, laser diode arrays, radars, and high-energy-laser mirrors (Weilin Qu and Issam Mudawar, 2002) [1]. Fluid flow in microchannels is a widely studied topic due to its critical importance in a large variety of engineering applications and scientific disciplines, such as microscale heat exchangers and reactors used in electronics, automotive vehicles, biochemistry, laser process equipments, and aerospace technology, etc (Liu et al, 2008) [2]. Pfund et al. (2000) measured the pressure drop, friction factor and Poiseuille number of water flowing along D_h = 128–1050 μm rectangular micro-channels, at Re = 60–3450. In the laminar regime (Re < 2000) their data show good agreement with the conventional theory with regard to the non-dependence of Poiseuille number on Reynolds number, but the measured values were higher than those corresponding to theoretical prediction [3]. Xu et al. (2000) considered liquid flow in 30–344 μm (hydraulic diameter) channels at Reynolds numbers of 20–4000, showed that characteristics of flow in microchannels agree with conventional behavior predicted by Navier–Stokes equations. They suggested that deviations from classical behavior reported in earlier studies may have resulted from errors in the measurement of microchannel dimensions, rather than any microscale effects

Received: February 2010
T. Sornakumar: Ph. D.

Nomenclature

A_c	cross section area of one microchannel (m^2)
A_s	surface area of one microchannel (m^2)
c_p	specific heat of water (J/Kg K)
D_h	hydraulic diameter of the microchannel (m)
f	friction factor
H_c	microchannel height or depth (m)
H	height or thickness of heat sink (m)
h	heat transfer coefficient (W/m^2 K)
I	current (A)
k	thermal conductivity of water (W/m K)
L	length of the heat sink/microchannel length (m)
m_t	total mass flow rate of the water coolant (kg/s)
m_c	microchannel mass flow rate (kg/s)
N	heat removed by water (W)
Nu	Nusselt number
n	number of microchannels
p	pressure (Pa)
Δp	pressure drop (Pa)
P	perimeter of microchannel (m)
Po	Poiseuille Number,
Q	heat input by the heater (W)
q	heat flux (W/m^2)
Re	Reynolds number
S	area of the heater top / area of the bottom of heat sink (m^2)
T_w	mean wall temperature (K or ^{0}C)
T	temperature of water (K or ^{0}C)
T_{in}	water inlet temperature (K or ^{0}C)
T_{out}	water outlet temperature (K or ^{0}C)
T_m	water mean temperature (K or ^{0}C)
ΔT	temperature difference of water (K or ^{0}C)
U_c	microchannel flow velocity (m/s)
V_c	microchannel volumetric flow rate (m^3/s)
V	voltage (V)
W_c	microchannel channel width (m)
W	width of heat sink (m)
W_{pp}	pumping power (W)

Greek Symbols

α_c	channel aspect ratio
ρ	density of water (kg/m^3)
μ	dynamic viscosity of water (Ns/m^2)
ν	kinematic viscosity of water (m^2/s)
θ	thermal resistance (K/W)

Subscripts

c	channel
exp	experimental
in	inlet
m	mean
out	outlet
th	theoretical
w	wall

[4]. An experimental investigation was conducted to explore the validity of classical correlations based on conventional sized channels for predicting the thermal behavior in single-phase flow through rectangular microchannels. The micro-channels considered ranged in width from 194 μm to 534 μm, with the channel depth being nominally five times the width in each case. Each test piece was made of copper and contained ten microchannels in parallel. The experiments were conducted with deionized water, with the Reynolds number ranging from approximately 300 to 3500. Numerical predictions obtained based on a classical, continuum approach were found to be in good agreement with the experimental data (showing an average deviation of 5%), suggesting that a conventional analysis approach can be employed in predicting heat transfer behavior in microchannels of the dimensions considered in this study. However, the entrance and boundary conditions imposed in the experiment need to be carefully matched in the predictive approaches (Poh-Seng Lee et al. 2005) [5].

Microscopic particle image velocimetry (microPIV) experiments were performed on square poly-dimethylsiloxane (PDMS) microchannels with hydraulic diameters ranging from 200 μm to 640 μm and for Reynolds numbers ranging from 200 through 3971. There was no evidence of early transition to turbulent, with transition observed at Reynolds numbers between 1718 and 1885 for the different sized microchannels. The flow was found to become fully turbulent at Reynolds numbers ranging from 2600 to 2900 (Hao Li and Michael G. Olsen, 2006) [6].

Liu and Garimella (2004) showed that conventional correlations offer reliable predictions for the laminar flow characteristics in rectangular microchannels over a hydraulic diameter range of 244–974 μm [7]. Steinke and Kandlikar (2006) reviewed the literature on single-phase liquid friction factors in microchannels and presented new experimental results of friction factor in microchannel with D_h = 8–990 μm. They reported that the experimental results showed good agreement in value and trend

with the conventional theory for laminar flow [8]. One potential solution to thermal management of a chip is to attach a micro-channel heat sink to inactive (back) side of the chip. Usually in a close-loop arrangement, coolant such as water is pumped through the micro-channels to remove the heat generated. Due to the small size of the micro-channels, the heat transfer coefficient is very high (Mishan et al. 2007) [9]. Kumaraguruparan et al. (2006) fabricated milling slitting saw type plain milling cutter. The fabricated milling cutter was mounted on the arbor of the universal milling machine and the microchannels were machined in a copper work piece to form the microchannel heat sink (MCHS). An experimental set-up was fabricated to place the microchannel heat sink on it and tests were conducted successfully [10].

Experimental procedure

Fabrication of milling slitting saw type plain milling cutter

The selection of cutter material depends upon the selection of the material for the microchannel heat sink. In this case Tool Steel D2 grade is selected as the cutter material to machine the microchannel. The D2 material is obtained in the form of round blank. The initial dimensions of the blank are 81 mm diameter and 20 mm thickness. The thickness of the blank is reduced to 2 mm by facing operation in a Lathe. The D2 Tool Steel blank is hardened by heating to 1025^0C, holding for 1 hour in a muffle furnace and quenched in air. Then the blank is tempered by heating to 540^0C, holding for 1 hour and cooled. The hardness of D2 Tool steel blank is 57 HRC. Subsequently, using a Tool and Cutter grinding machine, the teeth is cut on the D2 Tool Steel blank by setting primary and secondary relief angles. Totally 62 teeth are cut over the outer periphery of the D2 Tool Steel blank. The thicknesses of the teeth are reduced to 0.50 mm using a grinding wheel. The thickness except at the teeth is maintained as 2 mm. Thus the D2 Tool Steel slitting saw type plain milling cutter is fabricated. The details of the D2 Steel slitting saw type plain milling cutter is presented in table 1.

Table1 Slitting saw type plain milling cutter

Milling sawing cutter material	Tool Steel D2 Grade
Number of teeth	62
Diameter of the cutter	81
Primary relief angle	20 degrees
Secondary relief angle	40 degrees
Rake angle	3 degrees
Cutter width	0.50 mm

Microchannel fabrication

Aluminum is selected as the material for microchannel heat sink (MCHS) because of its high thermal conductivity. The fabricated milling slitting saw type plain milling cutter is mounted on the arbor of the horizontal milling machine. Aluminum block of length of 150 mm, breadth 100 mm and height 25 mm is used for manufacturing the MCHS. The aluminum block is held on the machine vice mounted on the table of the milling machine. The microchannels of 500 microns width and 5000 microns (5 mm) depth are machined in the aluminum work piece, to form the microchannel heat sink. The fin size between each microchannel is 1.5 mm. Thus 25 numbers of microchannels are machined in the aluminum work piece. The coolant used during the machining operation is soluble oil.

After completion of the microchannel machining, the aluminum block is held reverse for machining the pocket to house the heater. Commercial HSS end mill tool is used for pocketing the dimension of 130 mm length x 50 mm breadth x 7 mm depth. Five holes of 0.5 mm diameter were made in the heat sink below the channels to insert the thermocouples to measure the surface temperature of the block, by commercial HSS drills. The thermocouple holes were made at an interval of 20 mm alternatively on either side of the block i.e. three on one side and another two on the other side of block. Tapped drills were made on the top surface of the block along the sides of channels. With the tapped drills, the channels are sealed with acrylic sheet with help of fasteners. The drawing of the microchannel heat sink is shown in figure 1.

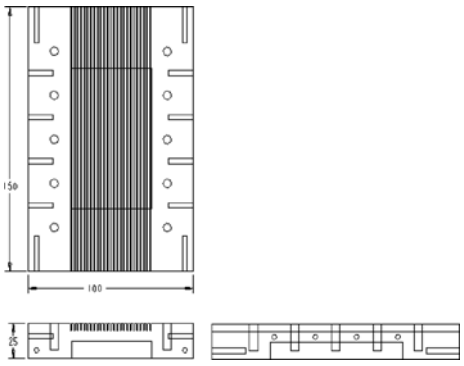

Fig. 1 Microchannel heat sink

Header Fabrication

Headers are used for ensuring steady and uniform fluid flow across the channels. Two headers for inlet and outlet respectively are fabricated with dimensions of 100 mm width x 25 mm thick x 25 mm length. Pocket of 5 mm depth, 10 mm width is made on each of the header. For each header, on both side of pocket through holes are

drilled for providing pressure probe and inlet/outlet nipples. Pressure sensors are fitted in this drilled hole in each header for measuring pressures in inlet and outlet plenums respectively. Thermocouple is also inserted in each header to measure the water inlet temperature and water outer temperature respectively by a 0.5 mm drilled hole on the other side. Then the two headers are assembled to the microchannel heat sink block with help of M6 Allen bolts. Then the acrylic sheet is placed over the MCHS block and fastened tightly.

Heater Fabrication

A heater is fabricated using nichrome wire as the heating element and mica as the electrical insulator. Coiled nichrome wire is wound on mica in such a way that the coils are present only on the top of mica. This is done to maximize the heat flow in one direction. The plate heater is designed to give a maximum output of 180 W.

Peristaltic Pump

Peristaltic pump is constant mass flow rate pump which can be used to pump any kind of fluid into the micro channels. The pump can supply the fluid at the rate of 110 to 900 ml per minute. The mass flow rate of the fluid can be varied by adjusting the knob provided in the pump.

Experimental Set-up

Totally 25 numbers of microchannels are machined in the aluminum substrate. The channels are separated by fins. The flow headers of rectangular cross section are separately fabricated and attached at both ends of the micro channels. To enable visualization, the top of the heat sink is covered with transparent acrylic plate. At the bottom of the heat sink a pocket is machined to insert the plate type heater. The bottom is closed with asbestos sheet to reduce the heat loss through the bottom. The MCHS assembled with both the inlet and outlet headers is shown in figure 2. The exploded view of the microchannel heat sink test set-up is shown in figure 3.

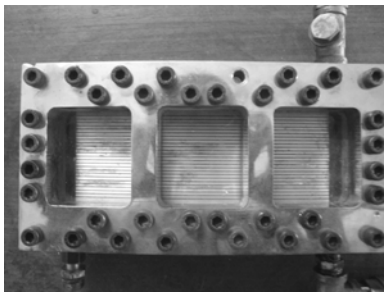

Fig.2 Photograph of the MCHS assembled with the headers

The inlet header and outlet header is provided with plenums for inlet and outlet so that when the water enters at inlet it first fills the tank and then passes through the microchannels that have been placed on the space provided. The flow through all the channels will be uniform and the outlet is collected at the outlet plenum and then goes out of the system. Calibrated iron-constantan thermocouples are inserted through the provisions provided in the two headers and the microchannel heat sink to measure wall temperatures and to measure the water inlet and outlet temperatures. The other ends of the thermocouples are connected to the temperature indicator. The top portion of the housing is covered using a transparent acrylic sheet to form flow passages and to visualize the flow. Metallic gaskets are provided at appropriate places to avoid any leakage from the housing. The heater is connected to the auto transformer to obtain the required heat input. The peristaltic pump is connected to the inlet port of the plenum of the inlet header. The mass flow rate of the coolant is varied by adjusting the flow control knob in the pump. The outlet port of the plenum of the outlet header is connected to the collecting tank. Figure 4 shows the schematic diagram of the complete experimental set-up. The photograph of the experimental set-up used in the present work is shown in figure 5. The ex-

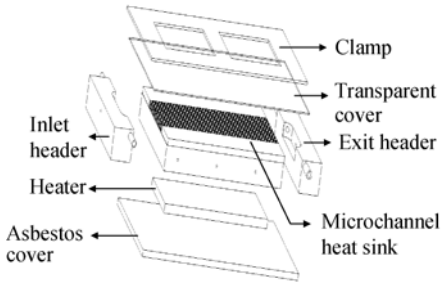

Fig.3 Exploded view of the microchannel heatsink experimental set-up

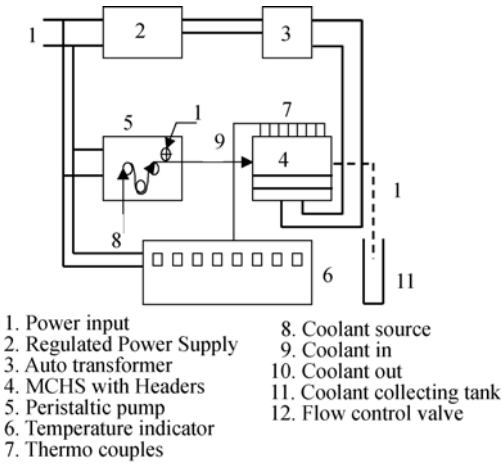

Fig.4 Schematic diagram of the experimental set-up

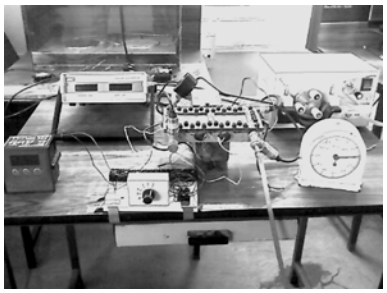

Fig.5 The photograph of the experimental set-up used in the present work

periments are conducted for various mass flow rates of the water coolant and various input heat flux. The water inlet temperature, water outlet temperature, wall temperature and pressure drop are noted. The water inlet temperature for all the experimental conditions is maintained constant at 25℃.

Results and discussion

Formulae

The channel aspect ratio α_c is:

$$\alpha_c = W_c / H_c \quad (1)$$

The cross section area of one microchannel A_c is :

$$A_c = H_c\ W_c \quad (2)$$

The surface area of one microchannel A_s is:

$$A_s = (2\ H_c + W_c)\ L \quad (3)$$

The perimeter of microchannel P is:

$$P = 2\ (H_c + W_c) \quad (4)$$

The hydraulic diameter D_h is:

$$D_h = 4\ A_c / P \quad (5)$$

The area of the heater top / area of the bottom of heat sink S is:

$$S = L\ W \quad (6)$$

The Heat input by the heater Q is:

$$Q = V\ I \quad (7)$$

The heat flux q is:

$$q = Q/S \quad (8)$$

The microchannel mass flow rate m_c is:

$$m_c = m_t/n \quad (9)$$

The microchannel velocity of flow U_c is:

$$U_c = m_c/(\rho A_c) \quad (10)$$

The microchannel volumetric flow rate V_c is:

$$V_c = m_c/\rho \quad (11)$$

The experimental temperature difference ΔT_{exp} is:

$$\Delta T_{exp} = (T_{out\ exp} - T_{in\ exp}) \quad (12)$$

The water mean temperature T_m is:

$$T_m = (T_{in\ exp} + T_{out\ exp})/2 \quad (13)$$

The kinematic viscosity ν is:

$$\nu = \mu/\rho \quad (14)$$

The Reynolds number of flow in the microchannel Re is:

$$Re = U_c D_h/\nu \quad (15)$$

The pressure drop across the microchannel Δp is:

$$\Delta p_{th} = (f\ L\ U_c^2\ \rho)/(2\ D_h) \quad (16)$$

The Poiseuille Number Po is given by:

$$Po = f_{th}\ Re = 24(1 - 1.3553\alpha_c + 1.9467\alpha_c^2 - 1.7012\alpha_c^3 + 0.9564\alpha_c^4 - 0.2537\alpha_c^5) \quad (17)$$

(Satish G. Kandlikar et al, 2006) [11].

The theoritical friction factor, f_{th} is:

$$f_{th} = Po/Re \quad (18)$$

The experimental friction factor f_{exp} is:

$$f_{exp} = (\Delta p_{exp}\ 2\ D_h)/(L\ U_c^2\ \rho) \quad (19)$$

The heat removed by water N is:

$$N = m_t\ c_p\ \Delta T_{exp} \quad (20)$$

The calculated heat transfer coefficient h is:

$$h = Q/[(T_w - T_m)A_s\ n\ L] \quad (21)$$

The calculated Nusselt number Nu is:

$$Nu = h\ D_h/k \quad (22)$$

The thermal resistance θ is:

$$\theta = (T_w - T_{in\ exp})/Q \quad (23)$$

The pumping power W_{pp} is:

$$W_{pp} = \Delta p_{th}\ V_c\ n \quad (24)$$

Variation of water properties with temperature

Water is used as working liquid in this simulation within the temperature range of liquid phase at atmospheric pressure, i.e., from 0 to 100 ^{0}C. The temperature dependency of density for liquid water ρ in Kg/m^3 is given as (McCutcheon et al. 1993) [12]:

$$\rho = 1000(1 - (T + 288.9414)\ /\ (508929.2*(T+68.12963))*(T-3.9863)^2 \quad (25)$$

where ρ is the density in kg/m^3 as and T is the temperature in ^{0}C.

The temperature dependency of dynamic viscosity for liquid water μ in kg/ms or Ns/m^2 is given as (Liu et al. 2008) [2]:

$$\mu(T) = \mu(T_{ref}) * (T/T_{ref})^n * \exp[B(T^{-1} - T^{-1}_{ref})] \quad (26)$$

where n = 8.9, B = 4700K, $\mu(T_{ref}) = 1.005\times10^{-3}$ kg/ms, T_{ref} = 293 K.

The temperature dependent thermal conductivity k in W/mK is given as (Liu et al. 2008) [2]:

$$k(T) = a_0 + a_1T + a_2T^2 + a_3T^3 \quad (27)$$

where $a_0 = -1.135$, $a_1 = 0.01154$, $a_2 = -2.375\times10^{-5}$ and $a_3 = 1.571\times10^{-8}$ and Temperature T is in K.

The temperature dependency of specific heat for liquid water c_p in J/kg K is given as,

$$c_p = (5348 - 7.42T + 1.17\times10^{-2}T^2) \quad (28)$$

where temperature T is in K (Hong et al. 2007) [13] for the temperature range of 283–373 K (the unit of temperature is K).

In general, constant thermophysical properties used in the analyses of previous work could not fully reveal the characteristics of fluid flow and heat transfer in the conditions of high heat flux and low Reynolds number flow, implying large variation of liquid properties, which is

always encountered in the applications of microchannels. For water in the temperature range from 0 to 100 ^{0}C, μ varies by 84% (decrease), k by 21% (increase), ρ by 4% (decrease) and c_p by 1% (nonmonotonic) (Wagner and Berlin, 1998) [14].

The experimental readings are presented in table 1. The water properties at the mean water temperature T_m is used for all the calculations. These values of variation of water properties with mean of the water temperature are used in all the calculations. The density increases with mass flow rate and decreases with input heat. The dynamic viscosity increases with mass flow rate and decreases with input heat. The thermal conductivity decreases with mass flow rate and increases with heat input. The specific heat increases with mass flow rate and decreases with input heat.

The variation of heat removed by water with mass flow rate, for different input heat is also presented in figure 6. The heat carried by the water increases with mass flow rate, since the heat transfer rate increase as water mass flow rate increases. However, increase of heat transfer rate is less than that of increase water mass flow rate. Therefore, outlet water temperature tends to decrease as water mass flow rate increases. The very good agreement between the electrical heat input and the heat removed by water proves virtually all the electrical power supplied by the heater was removed by the water, and heat losses are indeed negligible.

The variation of calculated heat transfer coefficient and Nusselt number with mass flow rate, for different input heat are presented in figure 7 and figure 8 respectively.

The heat transfer coefficient increases with mass flow rate, since the heat transfer rate increase as water mass flow rate increases. The heat transfer coefficient increases with increased heat input, due to higher temperature difference between inlet water temperature and heat sink wall temperature, because of the higher heat input into the system.

Table 1 The experimental readings

Total mass flow rate, m_t kg/s	$T_{out\ exp}$, ^{0}C	T_w, ^{0}C	Pressure drop, Δp_{exp}, Pa
Heat Input, 50 W			
0.002	30.50	38.10	49.40
0.0025	29.60	36.40	62.10
0.003	28.90	34.90	75.10
Heat Input, 100 W			
0.002	36.20	46.80	47.40
0.0025	34.30	43.90	59.20
0.003	32.80	42.30	72.10
Heat Input, 150 W			
0.002	41.90	51.70	44.70
0.0025	39.10	48.80	56.50
0.003	36.80	47.10	69.20

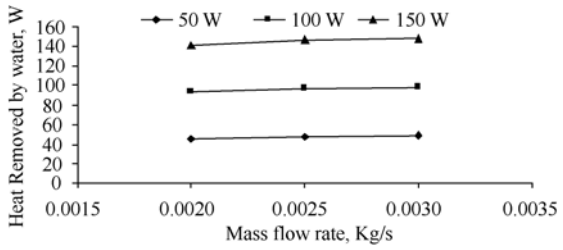

Fig.6 The variation of heat removed by water with mass flow rate m_t

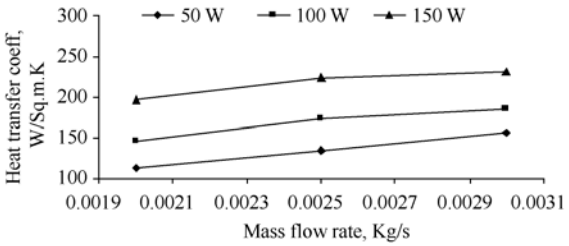

Fig.7 The variation of heat transfer coefficient h with mass flow rate m_t

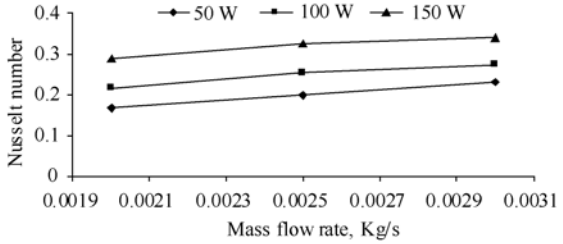

Fig.8 The variation of Nusselt number Nu with mass flow rate m_t

The Nusselt number also followed the same trend. The thermal performance of microchannels improved with higher Nusselt number.

The experimental and calculated theoretical pressure drops with respect to Reynolds number in the microchannels are plotted in figure 9. It can be seen that the pressure drop is linearly proportional to the Reynolds number, which indicates that all the flows are laminar, without any transition effects, as predicted by classical fluid dynamic theory.

The pressure drop decreases as applied heat input increases since the value of viscosity decreases as temperature increases for the same Reynolds number. The theoretical pressure drop accounts for the pressure drop along the microchannels, as well as the pressure losses associated with the abrupt contraction and expansion at the microchannel inlet and outlet, respectively. Figure 9 shows good agreement between the experimental and theoretical pressure drops.

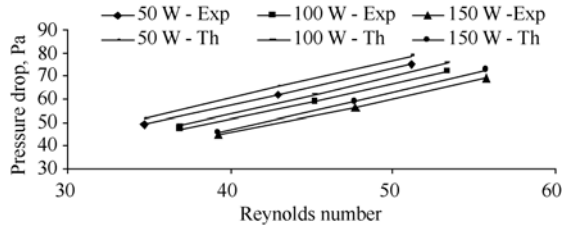

Fig.9 The variation of pressure drop with Reynolds number

The variation of friction factor with Reynolds number is presented in Figure 10. The experimental data for friction factor showed good agreement with macro channel laminar flow theory. The pressure drop in these microchannels increased and the friction factor decreased with increasing Reynolds number.

The variation of thermal resistance with pumping power for different input heat presented in Figure 11. For a case of constant thermal conductivity in the substrate and variable flow rate, a low thermal resistance value indicates a high convection coefficient between the substrate and the fluid. Conversely, high thermal resistance value indicates relatively weak convective transport.

The thermal performance is enhanced for higher mass flow rate and higher input heat. As the pumping power increase the thermal resistance decreases due to higher flow rate increasing the heat transfer rate. As the heat input increases the thermal resistance decreases due to higher heat transfer rate.

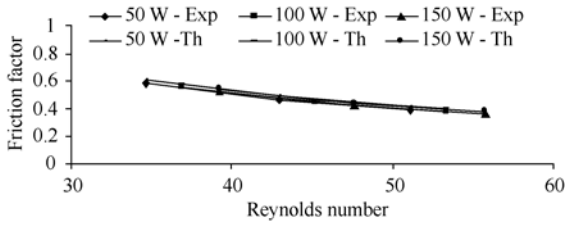

Fig.10 The variation of friction factor with Reynolds number

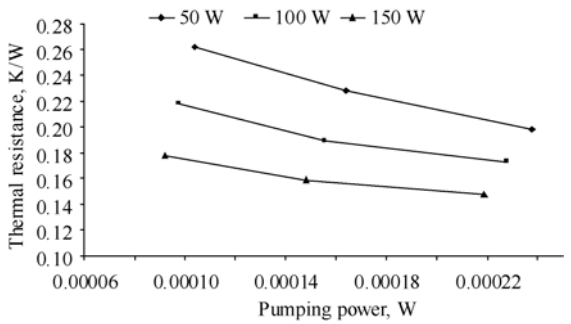

Fig.11 The variation of thermal resistance with pumping power

Conclusion

Microchannels are machined in aluminum work pieces to form the microchannel heat sink by a D2 grade Tool Steel milling slitting saw type plain milling cutter in a horizontal milling machine. A new experimental set-up has been fabricated to test the microchannel heat sink. The heat carried by the water increases with mass flow rate and heat input. The heat transfer coefficient and Nusselt number increases with mass flow rate and increased heat input. The pressure drop increases with Reynolds number and decreases with input heat. The friction factor decreases with Reynolds number and decreases with input heat. The thermal resistance decreases with pumping power and decreases with input heat.

References

[1] Weilin Qu, Issam Mudawar, Experimental and numerical study of pressure drop and heat transfer in a single-phase micro-channel heat sink, International Journal of Heat and Mass Transfer, 45 (2002) pp.2549–2565

[2] Liu, J.T., Peng, X.F., Wang, B.X., Variable-property effect on liquid flow and heat transfer in microchannels, Chemical Engineering Journal, 141 (2008) pp.346–353

[3] Pfund, D., Rector, D., Shekarriz, A., Popescu, A., Welty, J., Pressure drop measurements in microchannel, American Institute of Chemical Engineers Journal, 46 (2000) pp.1496–1507.

[4] Xu, B., Ooi, K.T., Wong, N.T., Choi, W.K., Experimental investigation of flow friction for liquid flow in microchannels, International communications in Heat and Mass Transfer, 27 (2000) pp.1165–1176.

[5] Poh-Seng Lee, Suresh V. Garimella, Dong Liu, Investigation of heat transfer in rectangular microchannels, International Journal of Heat and Mass Transfer, 48 (2005) pp.1688–1704.

[6] Hao Li, Michael G. Olsen, MicroPIV measurements of turbulent flow in square microchannels with hydraulic diameters from 200 μm to 640 μm, International Journal of Heat and Fluid Flow, 27 (2006) pp.123–134.

[7] Liu, D., Garimella, S.V., Investigation of liquid flow in microchannels, AIAA Journal of Thermophysics and Heat Transfer 18 (2004) pp.65–72.

[8] Steinke, M.E., Kandlikar, S.G., Single-phase liquid friction factors in microchannels, International Journal of Thermal Sciences, 45 (2006) pp.1073–1083.

[9] Mishan, Y., Mosyak, A., Pogrebnyak, E., Hetsroni, G., Effect of developing flow and thermal regime on momentum and heat transfer in micro-scale heat sink, International Journal of Heat and Mass Transfer, 50 (2007)

pp.3100–3114.

[10] Kumaraguruparan G., Sathish M., Sankara Subramaniam N., Sornakumar T., Design and Fabrication of Micro Channels for MEMS Applications, Journal of Synthesis and Reactivity in Inorganic, Metal-Organic, and Nano-Metal Chemistry, 36 (2006) pp.185-191.

[11] Satish G. Kandlikar, Single-Phase Liquid Flow in Minichannels and Microchannels, in: Heat Transfer and Fluid Flow in Minichannels and Microchannels, Authors: Satish G. Kandlikar, Srinivas Garimella, Dongqing Li, Stephane Colin, Michael R. King, Elsevier, Amsterdam, 2006, pp.87–136.

[12] McCutcheon, S.C., Martin, J.L, Barnwell, T.O. Jr. 1993, Water Quality, in: Handbook of Hydrology, (ed: Maidment, D.R), McGraw-Hill, New York, 1993.

[13] Hong, F.J., Cheng, P., Ge, H., Goh Teck Joo, Conjugate heat transfer in fractal-shaped microchannel network heat sink for integrated microelectronic cooling application, International Journal of Heat and Mass Transfer, 50 (2007) pp.4986–4998.

[14] Wagner, W., Berlin, A.K., Properties of water and steam: the industrial standard IAPWS-IF97 for the thermodynamic properties and supplementary equations for other properties, Springer-Verlag, New York, 1998.